Impact of Amorphous-C/Ni Multilayers on Ni-Induced Layer Exchange for Multilayer Graphene on Insulators

著者（英）	Hiromasa Murata, Noriyuki Saitoh, Noriko Yoshizawa, Takashi SUEMASU, Kaoru TOKO

journal or publication title	ACS Omega
volume	4
number	10
page range	14251-14254
year	2019-08

doi: 10.1021/acsomega.9b01708

ACS OMEGA

Article

Cite This: ACS Omega 2019, 4, 14251−14254

http://pubs.acs.org/journal/acsodf

Impact of Amorphous-C/Ni Multilayers on Ni-Induced Layer Exchange for Multilayer Graphene on Insulators

Hiromasa Murata,*,† Noriyuki Saitoh,‡ Noriko Yoshizawa,‡ Takashi Suemasu,† and Kaoru Toko*,†

†Institute of Applied Physics, University of Tsukuba, 1-1-1 Tennodai, Tsukuba, Ibaraki 305-8573, Japan

‡Electron Microscope Facility, TIA, AIST, 16-1 Onogawa, Tsukuba 305-8569, Japan

ABSTRACT: Layer exchange growth of amorphous carbon (a-C) is a unique technique for fabricating high-quality multilayer graphene (MLG) on insulators at low temperatures. We investigated the effects of the a-C/Ni multilayer structure on the quality of MLG formed by Ni-induced layer exchange. The crystal quality and electrical conductivity of MLG improved dramatically as the number of a-C/Ni multilayers increased. A 600 °C-annealed sample in which 15 layers of 4-nm-thick a-C and 0.5-nm-thick Ni were laminated recorded an electrical conductivity of 1430 S/cm. This value is close to that of highly oriented pyrolytic graphite synthesized at approximately 3000 °C. This improvement is likely related to the bond weakening in a-C due to the screening effect of Ni. We expect that these results will contribute to low-temperature synthesis of MLG using a solid-phase reaction with metals.

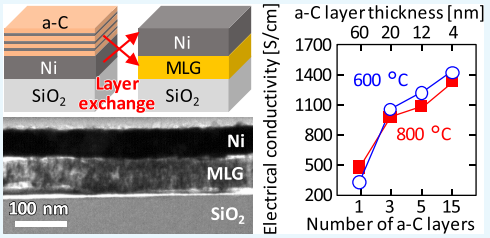

INTRODUCTION

The technology to synthesize graphene on arbitrary substrates is essential to combine advanced electronic devices and carbon materials.[1] Mechanical transfer has allowed for high-crystallinity graphene on insulators; however, concerns regarding imperfections in graphene, such as wrinkles, remain. This has motivated researchers to develop a transfer-free process for practical applications. Moreover, for devices which can endure large currents or heat, thick multilayer graphene (MLG) is preferable to few-layer graphene.[2−4] For example, low-resistance wiring requires a thickness of tens of nanometers to replace Cu wiring in large-scale integrated circuits, whereas a heat spreader requires a thickness of more than several micrometers, depending on the type of device. Vapor deposition techniques (e.g., chemical vapor deposition[5−10] and plasma-assisted vapor deposition[11,12]) are the most promising ways to grow MLG directly on insulators. However, forming thick, uniform MLG is difficult. Conversely, metal-induced solid-phase crystallization of amorphous carbon (a-C) or polymers has been actively studied for the direct synthesis of MLG on insulators.[13−27] Some of these techniques have enabled the synthesis of thick (>5 nm) MLG by controlling the initial thickness of a-C.[18−27] However, further investigations are required to achieve high-quality MLG on insulators.

Recently, we developed metal-induced layer exchange (MILE) of a-C.[28−32] In particular, MILE using Ni enabled us to synthesize uniform MLG at low temperature with a wide range of thicknesses.[29,32] Higashi et al. reported the effects of an a-Ge/Au multilayer structure on the layer exchange between Au and Ge.[33,34] The grain size of the resulting Ge layer was significantly improved by using the multilayer structure. The improvement was attributed to the diffusion of Ge atoms promoted by the bond weakening of a-Ge due to the screening effect.[35,36] In this study, we have applied the multilayer structure to the Ni-induced layer exchange of a-C, which has improved the crystal quality and electrical conductivity of the resulting MLG layer dramatically.

RESULTS AND DISCUSSION

Figure 1a shows the schematic of the sample preparation procedure. A Ni thin film (60 nm thickness) was prepared on quartz glass (SiO_2) substrates. Subsequently, a-C/Ni multilayers were prepared, where the number of a-C layers n was 1,

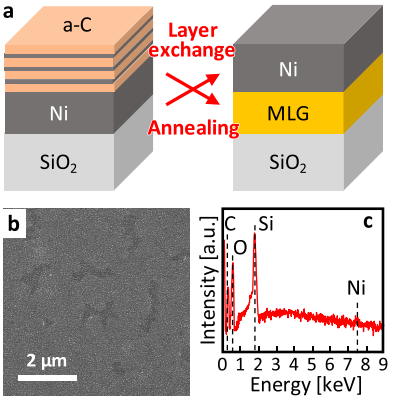

Figure 1. (a) Schematic of the sample preparation procedure. (b) Scanning electron microscopy (SEM) image and (c) energy dispersive X-ray (EDX) spectrum of the sample for n = 15 nm and t = 4 annealed at 600 °C after Ni removal. The EDX spectrum was obtained in a field of view of 1 mm square.

Received: June 10, 2019
Accepted: August 6, 2019
Published: August 20, 2019

DOI: 10.1021/acsomega.9b01708
ACS Omega 2019, 4, 14251−14254

3, 5, and 15. The thickness of the Ni layers between the a-C layers were fixed at 0.5 nm. Each a-C layer thickness t was 60 nm for n = 1, 20 nm for n = 3, 12 nm for n = 5, and 4 nm for n = 15, as summarized in Table 1. Therefore, the total thickness of a-C layers was fixed at 60 nm.

Table 1. Relationship between the a-C Thickness t and the Number of a-C Layers n[a]

t (nm)	60	20	12	4
n	1	3	5	15

[a]Total thickness of the a-C layer is 60 nm.

Figure 1b shows that MLG covers almost all of the substrate, although there are some voids. Such void formation can be suppressed by increasing the film thickness ratio of a-C to Ni.[30] Figure 1c shows the peaks corresponding to C, Si, and O. These elements originate from the MLG layer and SiO_2 substrate because the detection depth is greater than 1 μm in the energy dispersive X-ray (EDX) measurement. Note that the Ni concentration in the MLG layer is less than the EDX detection limit (~1%), which will be low enough not to contribute to the electrical conductivity σ. Such low metal contamination in the resulting layer is a typical feature of MILE, which is limited by solid solubility.[31]

We investigated the detailed cross-sectional structure of the sample for n = 15 and t = 4 annealed at 600 °C. The cross-sectional transmission electron microscopy (TEM) sample was prepared by the conventional focused ion beam method. The bright-field TEM image in Figure 2a and the elemental map in Figure 2b show that a single Ni layer is uniformly stacked on a single C layer. We note that there is no remnant of the a-C/Ni multilayer prepared on the upper part before annealing. The selected-area electron diffraction (SAED) pattern in Figure 2c reveals that C{002} planes in MLG are oriented almost parallel to the SiO_2 substrate. Compared to using a single a-C layer,[29] the current MLG has less ripple and higher quality. As shown in Figure 2d, the dark-field TEM image shows a bright contrast of the MLG layer in the entire region, which also indicates that MLG is highly (002) oriented. The high-resolution TEM image in Figure 2e shows that the lower part of MLG consists of small graphene layers, whereas Figure 2f shows that the upper part consists of relatively large graphene layers. The insertion of an AlO_x interlayer between the a-C/Ni multilayer and Ni will further improve the crystal quality of MLG.[30,32]

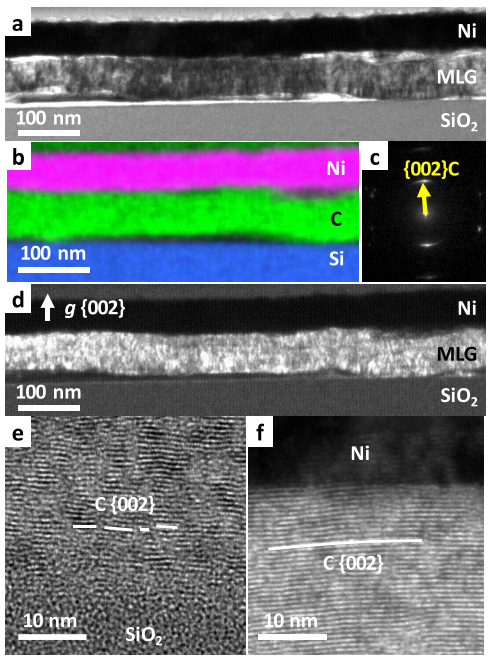

Figure 2. Characterization of the cross-section of the sample for n = 15 nm and t = 4 annealed at 600 °C before Ni removal. (a) Bright-field TEM image. (b) EDX elemental map. (c) SAED pattern taken from the region including the Ni and MLG layers with a selected area of 200 nm diameter. (d) Dark-field TEM image using the C{002} plane reflection. (e, f) High-resolution lattice images showing the (e) lower and (f) upper parts of the MLG layer, respectively.

Figure 3a shows that Raman spectra of the back side of the samples have peaks at approximately 1350, 1580, and 2700 cm^{-1}, corresponding to the disordered mode (D), graphitic mode (G), and D mode overtone (2D) peaks in the graphitic structure, respectively.[37] This means that layer exchange between the C and Ni layers occurred, and MLG formed on the SiO_2 substrate in all samples. The intensity ratio of the G to D peaks (I_G/I_D) in Raman spectra corresponds to the crystal quality of MLG.[37] Figure 3b shows that the I_G/I_D ratio increases as n increases for both annealing temperatures. The I_G/I_D ratio reaches the highest value of approximately 8 for the sample for n = 15 and t = 4 annealed at 600 °C. This result suggests that the crystal quality of MLG improves as n increases. According to previous studies on Au-induced layer exchange of Ge, the crystal quality improvement by the multilayer structure is attributed to the grain size enlargement due to the Ge diffusion enhancement.[33,34] Figure 3c indicates that σ also increases as n increases for both annealing temperatures. This behavior clearly reflects the crystal quality of the MLG found in the Raman study (Figure 3b). The 600 °C sample has a higher σ than the 800 °C sample for $n \geq 3$. This behavior is likely attributed to the larger grain size due to the lower growth temperature, which is well known for layer exchange. σ exhibits the maximum value of 1430 S/cm in a sample, where n = 15 and t = 4, annealed at 600 °C. This value is close to that of highly oriented pyrolytic graphite (1700 S/cm) synthesized at approximately 3000 °C. According to our previous paper,[32] σ can be improved to 2700 S/cm by inserting an AlO_x interlayer and controlling the MLG thickness. By combining these techniques, σ will further improve.

CONCLUSIONS

Adoption of the a-C/Ni multilayer structure greatly influenced the quality of MLG formed by layer exchange. The I_G/I_D ratio in Raman spectra and σ of MLG dramatically improved as the number of a-C/Ni multilayers increased. This behavior is likely because the higher number of multilayers provided the stronger screening effect and then the higher diffusion rate of C atoms into Ni, resulting in the larger grain size of MLG. Therefore, the present study is expected to contribute to low-temperature synthesis of MLG using solid-phase reaction with metals.

EXPERIMENTAL SECTION

Sample Preparation. All depositions were carried out using radio frequency (RF) magnetron sputtering (base pressure: 3.0 × 10^{-4} Pa) with Ar plasma. The substrate temperature was 200 °C for Ni and room temperature for a-C/Ni multilayer. The RF power was set to 100 W for a-C and 50

DOI: 10.1021/acsomega.9b01708
ACS Omega 2019, 4, 14251−14254

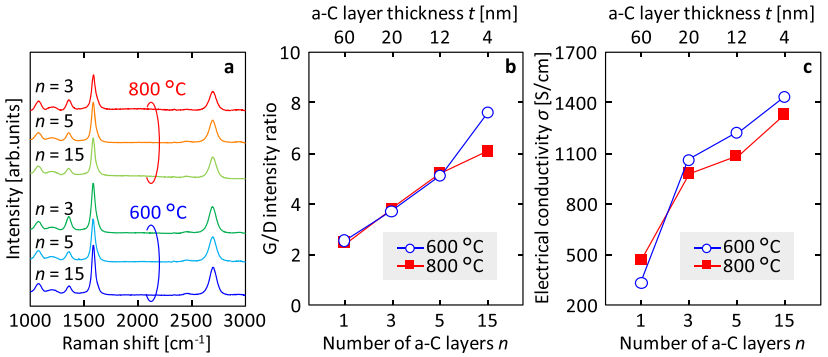

Figure 3. Raman study and the electrical properties of MLG formed by layer exchange. (a) Raman spectra obtained from the back side of the samples prior to Ni removal. (b) I_G/I_D ratio of the samples determined by the Raman spectra shown in (a), and (c) electrical conductivity σ of MLG after Ni removal, as a function of n and t.

W for Ni. The samples were annealed at 600 °C for 2 h and 800 °C for 10 min in ambient Ar to form MLG on the substrate by layer exchange. To remove the Ni that moved to the top layer, the sample was dipped in a diluted HNO_3 solution (2.0% HNO_3) for 10 min.

Material Characterization. Scanning electron microscopy (SEM) analyses and EDX spectroscopy were performed using Hitachi High-Technologies SU-8020 and JEOL JEO-2300. TEM analyses were performed using an analytical TEM, FEI Tecnai Osiris operating at 200 kV, equipped with an EDX spectrometer (FEI Super-X system). Raman spectroscopy was performed using JASCO NRS-5100, wherein the laser wavelength was 532 nm and the spot size was 5 μm. The σ was evaluated by the van der Pauw method using a Bio-Rad HL5500PC system and averaged over five measurements for each sample.

AUTHOR INFORMATION

Corresponding Authors

*E-mail: s1830090@s.tsukuba.ac.jp (H.M.).
*E-mail: toko@bk.tsukuba.ac.jp (K.T.).

ORCID

Hiromasa Murata: 0000-0002-7136-8131
Kaoru Toko: 0000-0002-3936-0519

Notes

The authors declare no competing financial interest.

ACKNOWLEDGMENTS

This work was financially supported by JSPS KAKENHI (No. 18K18844), JSPS Research Fellow (No. 18J20904), and Advanced Technology Institute Research Grants (RG2906). Some experiments were conducted at the International Center for Young Scientists at NIMS and the Nanotechnology Platform at the University of Tsukuba.

REFERENCES

(1) Novoselov, K. S.; Geim, A. K.; Morozov, S. V.; Jiang, D.; Zhang, Y.; Dubonos, S. V.; Grigorieva, I. V.; Firsov, A. A. Electric Field in Atomically Thin Carbon Films. *Science* **2004**, *306*, 666−669.

(2) Biswas, S.; Drzal, L. T. Multilayered Nano-Architecture of Variable Sized Graphene Nanosheets for Enhanced Supercapacitor Electrode Performance. *ACS Appl. Mater. Interfaces* **2010**, *2*, 2293−2300.

(3) Balandin, A. A. Thermal Properties of Graphene and Nanostructured Carbon Materials. *Nat. Mater.* **2011**, *10*, 569−581.

(4) Murali, R.; Yang, Y.; Brenner, K.; Beck, T.; Meindl, J. D. Breakdown Current Density of Graphene Nanoribbons. *Appl. Phys. Lett.* **2009**, *94*, No. 243114.

(5) Su, C.-Y.; Lu, A.-Y.; Wu, C.-Y.; Li, Y.-T.; Liu, K.-K.; Zhang, W.; Lin, S.-Y.; Juang, Z.-Y.; Zhong, Y.-L.; Chen, F.-R.; Li, L.-J. Direct Formation of Wafer Scale Graphene Thin Layers on Insulating Substrates by Chemical Vapor Deposition. *Nano Lett.* **2011**, *11*, 3612−3616.

(6) Kato, T.; Hatakeyama, R. Direct Growth of Doping-Density-Controlled Hexagonal Graphene on SiO_2 Substrate by Rapid-Heating Plasma CVD. *ACS Nano* **2012**, *6*, 8508−8515.

(7) Yen, W.-C.; Chen, Y.-Z.; Yeh, C.-H.; He, J.-H.; Chiu, P.-W.; Chueh, Y.-L. Direct Growth of Self-Crystallized Graphene and Graphite Nanoballs with Ni Vapor-Assisted Growth: From Controllable Growth to Material Characterization. *Sci. Rep.* **2015**, *4*, No. 4739.

(8) Murakami, K.; Tanaka, S.; Hirukawa, A.; Hiyama, T.; Kuwajima, T.; Kano, E.; Takeguchi, M.; Fujita, J. Direct Synthesis of Large Area Graphene on Insulating Substrate by Gallium Vapor-Assisted Chemical Vapor Deposition. *Appl. Phys. Lett.* **2015**, *106*, No. 093112.

(9) Chugh, S.; Mehta, R.; Lu, N.; Dios, F. D.; Kim, M. J.; Chen, Z. Comparison of Graphene Growth on Arbitrary Non-Catalytic Substrates Using Low-Temperature PECVD. *Carbon* **2015**, *93*, 393−399.

(10) Ueno, K.; Ichikawa, H.; Uchida, T. Effect of Current Stress during Thermal CVD of Multilayer Graphene on Cobalt Catalytic Layer. *Jpn. J. Appl. Phys.* **2016**, *55*, No. 04EC13.

(11) Liu, H.; Zhu, S.; Jiang, W. Rapid Flame Synthesis of Multilayer Graphene on SiO_2/Si Substrate. *J. Mater. Sci. Mater. Electron.* **2016**, *27*, 2795−2799.

(12) Park, H. J.; Ahn, B. W.; Kim, T. Y.; Lee, J. W.; Jung, Y. H.; Choi, Y. S.; Song, Y. I.; Suh, S. J. Direct Synthesis of Multi-Layer Graphene Film on Various Substrates by Microwave Plasma at Low Temperature. *Thin Solid Films* **2015**, *587*, 8−13.

(13) Peng, Z.; Yan, Z.; Sun, Z.; Tour, J. M. Direct Growth of Bilayer Graphene on SiO_2 Substrates by Carbon Diffusion through Nickel. *ACS Nano* **2011**, *5*, 8241−8247.

(14) Kwak, J.; Chu, J. H.; Choi, J.-K.; Park, S.-D.; Go, H.; Kim, S. Y.; Park, K.; Kim, S.-D.; Kim, Y.-W.; Yoon, E.; Kodambaka, S.; Kwon, S.-Y. Near Room-Temperature Synthesis of Transfer-Free Graphene Films. *Nat. Commun.* **2012**, *3*, No. 645.

(15) Banno, K.; Mizuno, M.; Fujita, K.; Kubo, T.; Miyoshi, M.; Egawa, T.; Soga, T. Transfer-Free Graphene Synthesis on Insulating Substrates via Agglomeration Phenomena of Catalytic Nickel Films. *Appl. Phys. Lett.* **2013**, *103*, No. 082112.

(16) Xiong, W.; Zhou, Y. S.; Hou, W. J.; Guillemet, T.; Silvain, J. F.; Gao, Y.; Lahaye, M.; Lebraud, E.; Xu, S.; Wang, X. W.; Cullen, D. A.; More, K. L.; Jiang, L.; Lu, Y. F. Solid-State Graphene Formation via a Nickel Carbide Intermediate Phase. *RSC Adv.* **2015**, *5*, 99037−99043.

(17) Berman, D.; Deshmukh, S. A.; Narayanan, B.; Sankaranarayanan, S. K. R. S.; Yan, Z.; Balandin, A. A.; Zinovev, A.;

DOI: 10.1021/acsomega.9b01708
ACS Omega 2019, 4, 14251−14254

Rosenmann, D.; Sumant, A. V. Metal-Induced Rapid Transformation of Diamond into Single and Multilayer Graphene on Wafer Scale. *Nat. Commun.* **2016**, *7*, No. 12099.
(18) Vishwakarma, R.; Rosmi, M. S.; Takahashi, K.; Wakamatsu, Y.; Yaakob, Y.; Araby, M. I.; Kalita, G.; Kitazawa, M.; Tanemura, M. Transfer Free Graphene Growth on SiO_2 Substrate at 250 °C. *Sci. Rep.* **2017**, *7*, No. 43756.
(19) Byun, S.-J.; Lim, H.; Shin, G.-Y.; Han, T.-H.; Oh, S. H.; Ahn, J.-H.; Choi, H. C.; Lee, T.-W. Graphenes Converted from Polymers. *J. Phys. Chem. Lett.* **2011**, *2*, 493−497.
(20) Gumi, K.; Ohno, Y.; Maehashi, K.; Inoue, K.; Matsumoto, K. Direct Synthesis of Graphene on SiO_2 Substrates by Transfer-Free Processes. *Jpn. J. Appl. Phys.* **2012**, *51*, No. 06FD12.
(21) Weatherup, R. S.; Baehtz, C.; Dlubak, B.; Bayer, B. C.; Kidambi, P. R.; Blume, R.; Schloegl, R.; Hofmann, S. Introducing Carbon Diffusion Barriers for Uniform, High-Quality Graphene Growth from Solid Sources. *Nano Lett.* **2013**, *13*, 4624−4631.
(22) Tamaoki, M.; Imaeda, H.; Kishimoto, S.; Mizutani, T. Transfer-Free Fabrication of Graphene Field Effect Transistor Arrays Using Solid-Phase Growth of Graphene on a SiO_2/Si Substrate. *Appl. Phys. Lett.* **2013**, *103*, No. 183114.
(23) Tanaka, H.; Obata, S.; Saiki, K. Reduction of Graphene Oxide at the Interface between a Ni Layer and a SiO_2 Substrate. *Carbon* **2013**, *59*, 472−478.
(24) Sato, M.; Takahashi, M.; Nakano, H.; Takakuwa, Y.; Nihei, M.; Sato, S.; Yokoyama, N. Intercalated Multilayer Graphene Wires and Metal/Multilayer Graphene Hybrid Wires Obtained by Annealing Sputtered Amorphous Carbon. *Jpn. J. Appl. Phys.* **2014**, *53*, No. 04EB05.
(25) Kosaka, M.; Takano, S.; Hasegawa, K.; Noda, S. Direct Synthesis of Few- and Multi-Layer Graphene Films on Dielectric Substrates by "Etching-Precipitation" Method. *Carbon* **2015**, *82*, 254−263.
(26) Zhuo, Q.-Q.; Wang, Q.; Zhang, Y.-P.; Zhang, D.; Li, Q.-L.; Gao, C.-H.; Sun, Y.-Q.; Ding, L.; Sun, Q.-J.; Wang, S.-D.; Zhong, J.; Sun, X.-H.; Lee, S.-T. Transfer-Free Synthesis of Doped and Patterned Graphene Films. *ACS Nano* **2015**, *9*, 594−601.
(27) Yamada, J.; Ueda, Y.; Maruyama, T.; Naritsuka, S. Direct Growth of Multilayer Graphene by Precipitation Using W Capping Layer. *Jpn. J. Appl. Phys.* **2016**, *55*, No. 100302.
(28) Murata, H.; Toko, K.; Suemasu, T. Multilayer Graphene on Insulator Formed by Co-Induced Layer Exchange. *Jpn. J. Appl. Phys.* **2017**, *56*, No. 05DE03.
(29) Murata, H.; Toko, K.; Saitoh, N.; Yoshizawa, N.; Suemasu, T. Direct Synthesis of Multilayer Graphene on an Insulator by Ni-Induced Layer Exchange Growth of Amorphous Carbon. *Appl. Phys. Lett.* **2017**, *110*, No. 033108.
(30) Murata, H.; Saitoh, N.; Yoshizawa, N.; Suemasu, T.; Toko, K. High-Quality Multilayer Graphene on an Insulator Formed by Diffusion Controlled Ni-Induced Layer Exchange. *Appl. Phys. Lett.* **2017**, *111*, No. 243104.
(31) Nakajima, Y.; Murata, H.; Saitoh, N.; Yoshizawa, N.; Suemasu, T.; Toko, K. Metal Catalysts for Layer-Exchange Growth of Multilayer Graphene. *ACS Appl. Mater. Interfaces* **2018**, *10*, 41664−41669.
(32) Murata, H.; Nakajima, Y.; Saitoh, N.; Yoshizawa, N.; Suemasu, T.; Toko, K. High-Electrical-Conductivity Multilayer Graphene Formed by Layer Exchange with Controlled Thickness and Interlayer. *Sci. Rep.* **2019**, *9*, No. 4068.
(33) Higashi, H.; Kasahara, K.; Kudo, K.; Okamoto, H.; Moto, K.; Park, J.-H.; Yamada, S.; Kanashima, T.; Miyao, M.; Tsunoda, I.; Hayama, K. A Pseudo-Single-Crystalline Germanium Film for Flexible Electronics. *Appl. Phys. Lett.* **2015**, *106*, No. 041902.
(34) Higashi, H.; Kudo, K.; Yamamoto, K.; Yamada, S.; Kanashima, T.; Tsunoda, I.; Nakashima, H.; Hamaya, K. Electrical Properties of Pseudo-Single-Crystalline Ge Films Grown by Au-Induced Layer Exchange Crystallization at 250 °C. *J. Appl. Phys.* **2018**, *123*, No. 215704.
(35) Hiraki, A. Low Temperature Reactions at Si/Metal Interfaces; What Is Going on at the Interfaces? *Surf. Sci. Rep.* **1983**, *3*, 357−412.
(36) Wang, Z. M.; Wang, J. Y.; Jeurgens, L. P. H.; Mittemeijer, E. J. Thermodynamics and Mechanism of Metal-Induced Crystallization in Immiscible Alloy Systems: Experiments and Calculations on Al/a-Ge and Al/a-Si Bilayers. *Phys. Rev. B* **2008**, *77*, No. 045424.
(37) Chu, P. K.; Li, L. Characterization of Amorphous and Nanocrystalline Carbon Films. *Mater. Chem. Phys.* **2006**, *96*, 253.

DOI: 10.1021/acsomega.9b01708
ACS Omega 2019, 4, 14251−14254